05 Oct 2022

Prototype Catalytic Membrane Reactor for Dimethyl Ether Synthesis Via Co2hydrogenation

Qiaobei Dong

Weiwei L. Xu

Xiao Fan

Huazheng Li

et. al. For a complete list of authors, see https://scholarsmine.mst.edu/che_bioeng_facwork/1027

Recommended Citation

Q. Dong and W. L. Xu and X. Fan and H. Li and N. Klinghoffer and T. Pyrzynski and H. S. Meyer and X. Liang and M. Yu and S. Li, "Prototype Catalytic Membrane Reactor for Dimethyl Ether Synthesis Via Co2hydrogenation," *Industrial and Engineering Chemistry Research*, vol. 61, no. 39, pp. 14656 - 14663, American Chemical Society, Oct 2022.
The definitive version is available at https://doi.org/10.1021/acs.iecr.2c02851

I&EC research
Industrial & Engineering Chemistry Research
pubs.acs.org/IECR
Article

Prototype Catalytic Membrane Reactor for Dimethyl Ether Synthesis via CO_2 Hydrogenation

Qiaobei Dong, Weiwei L. Xu, Xiao Fan, Huazheng Li, Naomi Klinghoffer, Travis Pyrzynski, Howard S. Meyer, Xinhua Liang, Miao Yu, and Shiguang Li*

Cite This: *Ind. Eng. Chem. Res.* 2022, 61, 14656−14663

Read Online

ACCESS | Metrics & More | Article Recommendations

ABSTRACT: Dimethyl ether (DME) has become attractive as a potential environmentally friendly substitute for diesel and liquefied petroleum gas (LPG) due to its similar properties to those of LPG, high cetane number, but less carbon emissions. In this work, we developed a novel prototype-scale catalytic membrane reactor to synthesize DME directly from CO_2 and renewable H_2, which could address the environmental and fuel security issues in a cost-effective way. This membrane reactor was equipped with superior hydrophilic NaA zeolite membranes and bifunctional Cu−ZnO−ZrO_2−Al_2O_3/HZSM-5 catalysts. The effects of the reaction temperature and gas hourly space velocity (GHSV) on the DME synthesis were investigated. Compared with the fixed bed catalytic reactor, the catalytic membrane reactor with a unique NaA membrane significantly enhanced the DME yield and CO_2 conversion from 8.71 and 21.4 to 22.8 and 33.7%, respectively. The highest DME production rate of 1.31 kg/day was achieved at 300 °C and a GHSV of 8400 mL/(g·h). This work demonstrates the feasibility of the catalytic membrane reactor for DME production via CO_2 hydrogenation as an approach to market readiness.

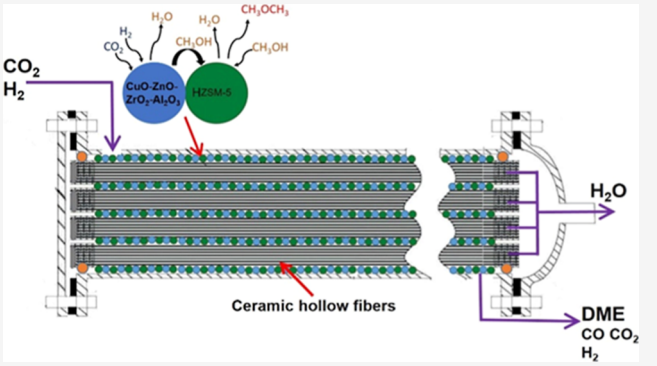

1. INTRODUCTION

The rapidly increased CO_2 concentration in the atmosphere due to anthropogenic activities leads to the rising temperature of the earth and results in awful climate change.[1] According to the measurement in 2020, the atmospheric CO_2 level has exceeded 417 ppm,[2] and the average global temperature has increased by at least 1.1 °C since the Industrial Revolution.[3] Although various attempts, such as replacing fossil resources by renewable energy,[4] process intensification,[5] or development of measures to increase energy efficiency,[6] have been made to reduce the greenhouse gas emissions, disruptive changes, such as carbon capture and utilization, are still required to further reduce the greenhouse gas emissions to mitigate global warming.[7−9] Among various CO_2 utilization approaches, catalytic hydrogenation of CO_2 to valuable chemicals and fuels, such as dimethyl ether (DME), is considered as one promising direction.[10−12] As a clean prospective "future fuel", DME has a high cetane number, similar properties as those of liquefied petroleum gas (LPG) under ambient conditions, and generates less emissions, such as no sulfur oxide or soot release during combustion.[13] All of these make DME attractive for substituting diesel with no changes needed in exiting engines,[14] replacing LPG for household using, or working as raw materials for producing a wide range of chemical building blocks.[15]

DME is typically synthesized through two approaches: (1) in a two-step process, methanol is first produced and then converted into DME through dehydration; (2) in a one-step process, DME is synthesized directly from syngas in a single reactor, where the feed gas can be replaced by a CO_2/H_2 mixture.[14] Compared with the two-step process, the one-step DME synthesis from CO_2 and H_2 is more promising due to direct CO_2 utilization. This one-step process combines methanol production via CO_2 hydrogenation, methanol dehydration, and reverse water gas shift as side reactions

$$CO_2 + 3H_2 \rightarrow CH_3OH + H_2O \quad \Delta H = -49.5\ \text{kJ/mol} \tag{1}$$

$$2CH_3OH \rightarrow CH_3OCH_3 + H_2O \quad \Delta H = -23.4\ \text{kJ/mol} \tag{2}$$

Received: August 9, 2022
Revised: September 14, 2022
Accepted: September 16, 2022
Published: September 26, 2022

https://doi.org/10.1021/acs.iecr.2c02851
Ind. Eng. Chem. Res. 2022, 61, 14656−14663

$$CO_2 + H_2 \rightleftharpoons CO + H_2O \qquad \Delta H = +41.2\ \text{kJ/mol} \tag{3}$$

However, the first reaction of methanol synthesis from CO_2/H_2 is severely limited by the equilibrium. Combining the two reactions in one reactor using a bifunctional catalyst can alleviate this issue because in situ methanol consumption can shift the equilibrium toward to DME production and lower operating cost.[16] A bifunctional catalyst with metal and acid functions is needed to conduct methanol synthesis and methanol dehydration reaction.[17−22] In this catalytic system, water is one of the major byproducts and has an exponential negative effect on the overall catalytic performance because the catalyst activity is inhibited as water adsorbed on its surface, resulting in Cu NPs sintering and, thus, leading to reduced CO_2 conversion and low DME yield.[23−25] If the produced water is removed in situ during the DME synthesis process, the deactivation of catalyst could be alleviated; meanwhile, the reaction equilibrium could be pushed toward the product formation side. This concept has been confirmed by several simulation studies.[26−29] Therefore, developing a novel catalytic membrane reactor equipped with a water removal membrane could be an effective way to overcome the catalyst deactivation and shift the equilibrium toward a higher CO_2 conversion into DME for the one-step DME synthesis process.

Inorganic membranes, especially hydrophilic zeolite membranes have been widely employed in removing water from other molecules owing to their high thermal stability and water permeability,[30−32] and some studies have demonstrated that employing the water removal zeolite membrane could benefit the dehydration of methanol to form DME.[33−35] However, as for the one-step DME synthesis process, there are few experimental works. Most of them are simulation studies and conducted to investigate the potential of the water removal membrane for the enhancement of DME yield.[32,34,36,37] For example, by using a small catalyst bed with an inner diameter of 9.5 mm and a length of 70 mm, Rodriguez-Vega et al. demonstrated the benefit of using a membrane reactor equipped with a LTA zeolite membrane to boost the DME yield from 2.8 to 6.57% and CO_2 conversion from ∼22.5 to 35% under 325 °C with good catalyst stability.[38] However, the major obstacle for applying the water removal membrane in large-scale DME synthesis is the low water selectivity because structural defects are almost inevitable from the zeolite membrane synthesis,[39,40] which leads to the loss of reactants or products, such as CO_2, H_2, MeOH, CO, and DME, by permeating through the membranes with water. In general, the experimental research on direct converting CO_2 and H_2 into DME by using a membrane reactor is still in its infancy. Most of the investigations have been conducted in the laboratory scale. It still is a big challenge to advance the maturity level for this technology.

In our previous work, a superior water-selective NaA zeolite membrane was developed, which showed H_2O/CO_2, H_2O/H_2, H_2O/CO, and H_2O/MeOH selectivity as high as 551, 190, 170, and 80, respectively, under 21 bar at 250 °C.[41] Conventional Cu/Zn/Al (CZA) was widely used for CO_2 hydrogenation because of the high activity; however, its stability is not sufficient. Therefore, the CuO/ZnO/ZrO_2/Al_2O_3 (CZZA) catalyst was developed which has Zr as a structure promoter to improve the catalyst stability.[18] The bifunctional CZZA/HZMS-5 catalyst was synthesized and tested in a fixed bed reactor,[20] which showed CO_2 conversion as high as 26.2% and DME yield of 18.3% under 28 bar at 240 °C. By combining the superior water-selective NaA zeolite membrane and the bifunctional CZZA/HZSM-5 catalyst, a lab-scale catalytic membrane reactor showed a significantly improved performance with CO_2 conversion increased up to 73.4% and DME yield increased to 54.5%.[42] Herein, a highly efficient prototype-scale membrane reactor was designed and tested under different operating conditions for DME direct synthesis from CO_2 hydrogenation to push the technology readiness level for the DME synthesis membrane reactor to a higher level.

2. EXPERIMENTAL METHODS

2.1. Catalyst Preparation. In the CuO/ZnO/ZrO_2/Al_2O_3 (CZZA) catalyst preparation process, zinc nitrate [$Zn(NO_3)_2$·$6H_2O$, 98%], copper nitrate [$Cu(NO_3)_2$·$3H_2O$, 99%], zirconium dinitrate oxide hydrate [$ZrO(NO_3)_2$·xH_2O, 99%], and aluminum nitrate [$Al(NO_3)_3$·$9H_2O$, 98%] were used as metal precursors. Sodium carbonate (Na_2CO_3, 99%) was used as the precipitant. Commercial ammonia-ZSM-5 catalyst (SiO_2/Al_2O_3 = 23:1 molar ratio, surface area of 425 m^2/g) was used for the preparation of HZSM-5 catalyst. All chemicals were obtained from Alfa Aesar (USA).

CZZA catalyst was synthesized by the co-precipitation method and its atomic ratio was optimized as Cu/Zn/Zr/Al = 4:2:1:0.5, followed by a procedure that we developed previously.[18,20] Typically, 0.4 M aqueous solutions of different metal nitrates including $Cu(NO_3)_2$, $Zn(NO_3)_2$, $Al(NO_3)_3$, and $ZrO(NO_3)_2$ were mixed together and this solution was added dropwise to the preheated deionized (DI) water (400 mL, 65−70 °C) in a beaker. Meanwhile, an aqueous solution of Na_2CO_3 with the same precursor concentration was added simultaneously to the same beaker under vigorously stirring. The precipitation of all metal precursors into the form of hydrocarbonate took around one and a half hour. An sodium carbonate solution was used to adjust the pH of mixed solution to 7.0 in the end of co-precipitation, and then, an aging process was initiated under a constant temperature of 70 °C for 30 min. Lastly, DI water was used to rinse the precipitates several times in a funnel, and the precipitates were filtered and followed by overnight at 110 °C in an oven, and subsequently calcined at 400 °C for 5 h to be transformed into metal oxides. The commercial ammonia-ZSM-5 was calcined in a muffle furnace at 500 °C in air for 5 h to obtain the HZSM-5 catalyst.

2.2. DME Synthesis in Fixed Bed Reactor. A high-pressure fixed-bed stainless steel reactor was used for evaluating the catalytic performance of the CZZA/HZSM-5 bifunctional catalyst for CO_2 hydrogenation to DME. The I.D. and O.D. of this reactor are 9.5 and 12.7 mm, respectively. According to our previous study,[18] the mass ratio of CZZA and HZSM-5 was 0.5 g:0.5 g. Prior to the tests, the bifunctional catalysts were first reduced at 250 °C for 3 h under a hydrogen environment at atmospheric pressure. Subsequently, the catalytic measurements were carried out under 240 °C and 2.8 MPa through feeding the reactant gases H_2/CO_2 with a molar ratio of 3:1 at a flow rate of 24 mL/min [gas hourly space velocity (GHSV) = 1440 mL/(g·h)]. A thermocouple was inserted inside the reactor tube to measure the temperature, and the reaction pressure was controlled by a back-pressure regulator. GC (gas chromatography, SRI 8610C) equipped with a two-column separation system (a 6-foot HAYESEP-D column and a 6-foot molecular sieve 13X

https://doi.org/10.1021/acs.iecr.2c02851
Ind. Eng. Chem. Res. 2022, 61, 14656−14663

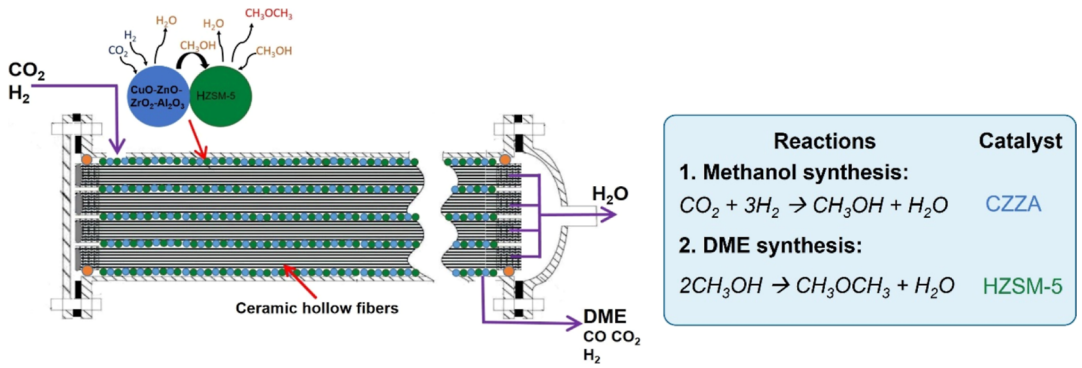

Figure 1. Schematic diagram of the catalytic membrane reactor with bifunctional catalyst showing one-step DME synthesis from CO_2 and H_2.

column connected to a flame ionization detector and thermal conductivity detector) was used for analyzing the product.

2.3. Membrane Preparation. Na^+-gated nanochannel membrane preparation followed the procedure that was reported in our previous work.[41] Basically, ceramic hollow fibers were dip-coated in a NaA seed solution (1 wt %, seed size of 50−250 nm) and subsequently transferred to an oven for drying at 200 °C overnight. A gel solution with a molar composition of $Al_2O_3/5SiO_2/50Na_2O/1000H_2O$ was prepared by mixing sodium aluminate ($NaAlO_2$, Al_2O_3: 50−56 wt %, Na_2O: 37−45 wt %, Sigma-Aldrich), Ludox colloidal (40 wt % in water, Sigma-Aldrich), and sodium hydroxide (NaOH, 98 wt %, Sigma-Aldrich) in DI water. The seeded hollow fibers were soaked in the gel solution at 80 °C for 5 h. After the hydrothermal synthesis, the membrane was washed thoroughly and dried for use in the membrane reactor.

2.4. DME Synthesis in Membrane Reactor. Seven hollow fiber membranes with a length of 15 cm were installed into the reactor. These membranes with such a membrane area are sufficient for removing the produced water during the reaction. The bifunctional catalyst (150 g) was prepared by mixing CZZA and HZSM-5 with a mass ratio of 5:1. The catalyst was first reduced with a H_2/N_2 mixture flow (H_2/N_2 volumetric flow rate ratio 1:2) for 12 h at 220 °C. Before the DME synthesis reaction, N_2 was applied to purge the whole system until the target operation temperature was reached. Then, the feed CO_2/H_2 mixture (CO_2/H_2 volumetric flow rate ratio 1:3) was introduced into the reactor for DME synthesis. The pressure of the membrane reactor was maintained at 550 psig during the test. The membrane reactor performance was reflected by parameters which could be calculated by following equations

$$X_{co_2} = \frac{n_{CO_2in} - n_{CO_2out}}{n_{CO_2in}} \times 100\% \quad (4)$$

$$Y_{DME} = \frac{2 \times n_{DME}}{n_{CO_2in}} \times 100\% \quad (5)$$

$$Y_{CO} = \frac{n_{CO}}{n_{CO_2in}} \times 100\% \quad (6)$$

$$Y_{MeOH} = \frac{n_{MeOH}}{n_{CO_2in}} \times 100\% \quad (7)$$

where X_{CO_2} is CO_2 conversion and Y_{DME}, Y_{CO}, and Y_{MeOH} are the yields of DME, CO, and MeOH, respectively. n_{CO_2}, n_{DME}, n_{CO}, and n_{MeOH} are the moles of CO_2, DME, CO, and MeOH, respectively. Meanwhile, n_{CO_2} was further specifically divided into n_{CO_2in} and n_{CO_2out}, representing the CO_2 feed in and out from the system.

2.5. Characterization. X-ray diffraction (XRD) patterns were obtained from a Philips X'Pert PRP PW3050 X-ray diffractometer instrument equipped with a Cu Kα radiation and a graphite generator. The scanning range is 5−90° and the scanning rate is 0.5°/min. Transmission electron microscopy (TEM) images were acquired using a 300 kV FEI Tecnai F30 TEM instrument. The surface and cross-sectional scanning electron microscopy (SEM) images were collected by a Carl Zeiss AURIGA CrossBeam instrument.

3. RESULTS AND DISCUSSION

3.1. DME Membrane Reactor and Testing System. The schematic diagram of the catalytic membrane reactor for one-step DME synthesis is shown in Figure 1. The CO_2/H_2 mixture was introduced into the catalytic membrane reactor as feed stock for one-step direct DME production. The bifunctional CZZA/HZSM-5 catalyst is filled in the outside void between hollow fibers. Two major reactions, including methanol production and DME synthesis, occurred simultaneously in the membrane reactor. To improve CO_2 conversion and catalyst performance, byproduct water was removed in situ through NaA zeolite membranes that grew on the external surface of the hollow fibers. The hydrophilic nature of the NaA results in strong adsorption of water into the pores of the membrane, and the water condensed in pores transports through the membrane by capillary action forces, enabling the removal of water while blocking the transportation of other small molecule gases through membrane pores. This is expected to increase the reaction kinetics by reducing the catalyst deactivation caused by water absorption and pushing the reaction equilibrium toward higher product formation.

3.1.1. Prototype-Scale Catalytic Membrane Reactor. To advance the technology maturity level for the one-step DME synthesis process, a prototype catalytic membrane reactor was designed based on the previous lab-scale membrane reactor. As shown in Figure 2A, the membrane stub was fabricated on a blind flange, and seven channels with a diameter of 5.8 mm were drilled out for the installation of hollow fiber membranes with a diameter of 5.7 mm. The hollow fiber membranes were sealed in the membrane stub channels by using house-made hollow nuts and O-ring (Figure 2B). The membrane housing was constructed by welding one 1.5 in. pipe in length of 12 in. together with two raised surface flanges, and a 0.325 in. hole was drilled out on the housing, on which a 3/8 in. tubing

https://doi.org/10.1021/acs.iecr.2c02851
Ind. Eng. Chem. Res. 2022, 61, 14656−14663

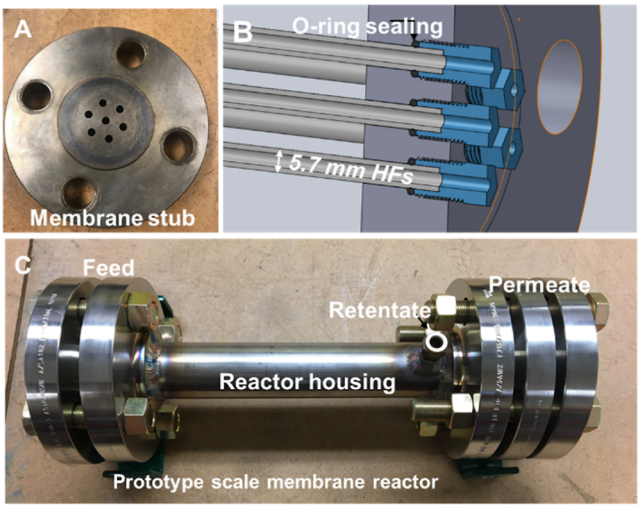

Figure 2. Design of the prototype-scale bifunctional catalytic membrane reactor: (A) picture of the membrane stub in which seven hollow fiber membranes can be installed; (B) 3D cross-sectional view of the membrane reactor with O-ring sealing; and (C) picture of the prototype-scale membrane reactor.

adaptor was welded as the outlet for products (retentate); two blind flanges were used for reactor sealing, one 0.325 in. hole was drilled out on each flange, and 3/8 in. adaptors were welded as gas inlet for feed side and outlet for permeate, respectively. As shown in Figure 2C, the membrane reactor was composed by four parts, feed, reactor housing, permeate, and membrane stub which was sandwiched between the membrane housing and permeate. After assembling all four parts with bolts and sealed with graphite gaskets, the membrane reactor was installed into the furnace for testing. During the test, generated water was removed from the reactor by permeating through the membrane and the hollow nuts to the permeate side.

3.1.2. Prototype Scale DME Synthesis System. The prototype testing system was home-designed and built, and the process flow diagram and picture of the prototype-scale DME synthesis system are shown in Figure 3. The flow rates of the feed gases, CO_2 and H_2, were regulated by mass flow controllers. The feed gas mixture was heated through the top preheat furnace and then introduced into a membrane reactor for DME production. The membrane reactor was sat in the bottom reactor furnace, and the temperature of the furnace was set to the desired catalytic reaction temperature. The pressure of the membrane reactor was controlled by a back-pressure regulator connected to the retentate side, and a vacuum pump was connected to permeate side to provide the driving force for the water removal through the membrane. Pressure transducers were used to monitor the pressure of feed, retentate, and permeate side. Besides, to prevent any water condensation in the pipelines, both retentate and permeate lines were heat traced with a setting temperature of 180 °C. Methanol, mostly in retentate line, and water, mostly in permeate line, produced in the DME synthesis process were condensed and collected separately in a chiller. The testing system was program controlled by a LabVIEW software (National Instruments). The gas compositions for retentate and permeate were analyzed by a micro-GC (Varian Inc. CP-4900). GC calibration was conducted periodically to enable accurate reading.

3.2. Catalyst Characterization and Catalytic Performance. The morphological properties of the reduced CZZA catalyst were characterized by TEM. As shown in Figure 4A, nanoparticles (less than 100 nm) are evenly distributed without obvious agglomeration. As shown in Figure 4B, for the CZZA/HZSM-5 catalyst, the CuO characteristic diffraction peaks appeared at 2θ = 35.5 and 38.7° correspond to the (002) and (111) crystal planes of tenorite, and the diffraction peaks at 2θ = 31.8 and 56.6° correspond to the (100) and (002) planes of ZnO, respectively. The ZrO_2 and Al_2O_3 diffraction peaks were not observed because of their amorphous state or low weight percentage in the catalyst. Three diffraction peaks at 23.0, 23.8, and 24.2°, respectively, correspond to the (501), (151), and (303) crystal faces of the HZSM-5 catalyst.

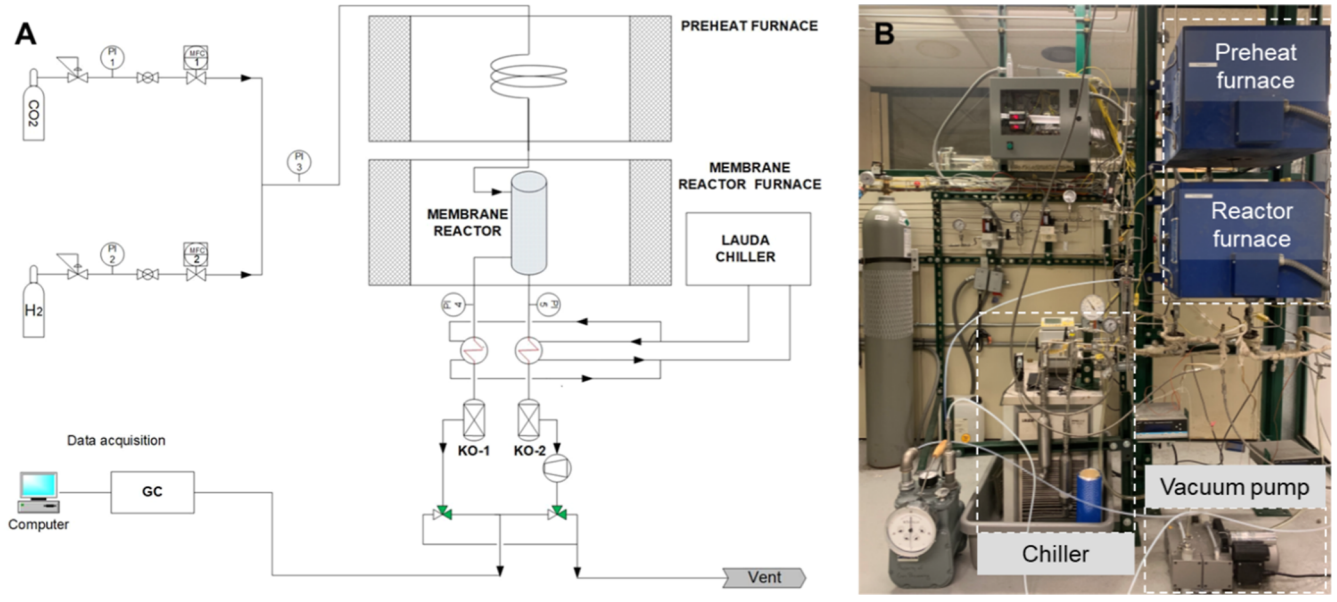

Figure 3. (A) Process flow diagram and (B) picture of the prototype-scale DME synthesis system.

https://doi.org/10.1021/acs.iecr.2c02851
Ind. Eng. Chem. Res. 2022, 61, 14656−14663

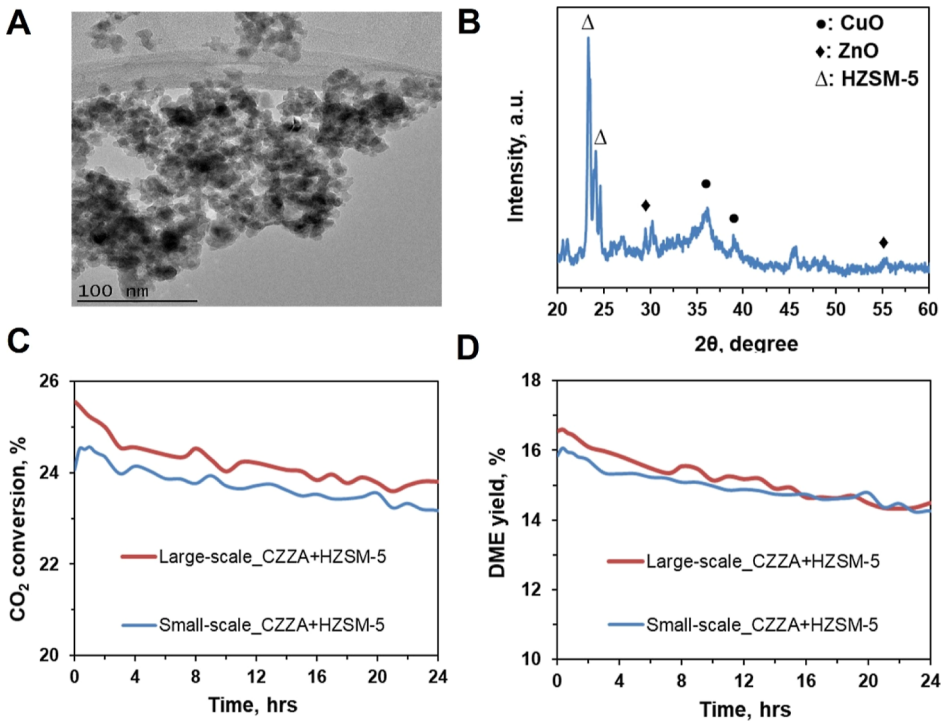

Figure 4. (A) TEM image of the CZZA catalyst; (B) XRD pattern of CZZA/HZSM-5 bifunctional catalysts; (C) CO_2 conversion; and (D) DME yield of small-scale and large-scale one-step DME synthesis over CZZA/HZSM-5 bifunctional catalysts.

The experimental results of large-scale (i.e., 100 g per batch) and small-scale (i.e., 15 g per batch) batch of CZZA catalysts mixed with HZSM-5 for CO_2 DME synthesis directly from CO2 hydrogenation under the operating conditions [240 °C, 2.8 MPa, GHSV = 1440 mL/(g·h)] are summarized in Figure 4C,D. We found that the catalytic performance of these two different batch sizes of CZZA catalysts were very close to each other, demonstrating that our prepared CZZA catalyst can be synthesized through mass production while maintaining good catalytic activity.

3.3. Membrane Morphology and Structure. The Na^+-gated nanochannel membranes were synthesized on ceramic hollow fiber substrates (I.D. of 3.5 mm, O.D. of 5.7 mm, length of 250 mm) by following the procedures described in previously report.[41] The surface morphology of the as-prepared membrane was characterized by SEM, as shown in Figure 5A; continuous and dense membrane layers were grown on the outer surface of ceramic follow fibers. Figure 5B shows the cross-sectional view of the hollow fiber, indicating that the average membrane thickness was around 2−4 μm. The structure of the as-prepared membrane was characterized by XRD and compared with the standard diffraction pattern of NaA, as shown in Figure 6 (red pattern), only NaA and alumina characteristic peaks were detected, indicating that no impurity in the membrane layer and pure NaA membrane layer were obtained.

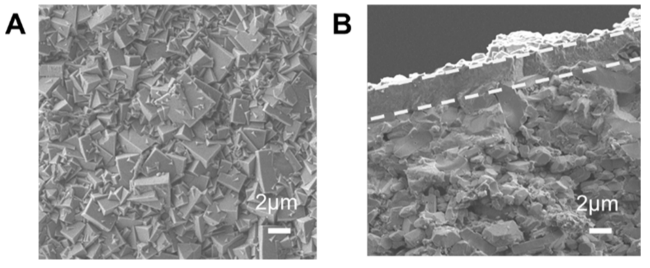

Figure 5. (A) Surface and (B) cross-sectional SEM images of the NaA membrane.

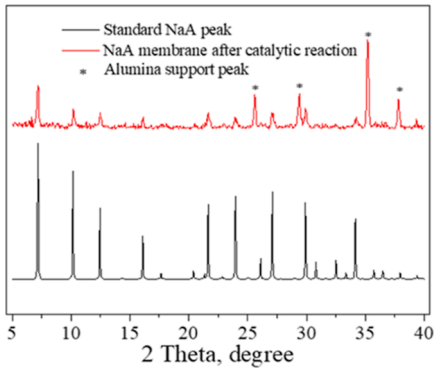

Figure 6. XRD patterns of NaA membrane before and after catalytic reaction.

3.4. Prototype Scale DME Synthesis Testing. Figure 7 shows the results of DME, CO, MeOH yield, and CO_2 conversion of the traditional fixed bed reactor and the prototype-scale membrane reactor under different operating temperatures at a GHSV of 1400 mL/(g·h). In the fixed bed reactor, the DME yield was 3.39% at 240 °C, and as the operating temperature increased to 300 °C, the DME yield increased to 7.91% with CO_2 conversion increased from 13.5 to 23.2%. However, the MeOH yield decreased from 5.07 to 3.69%, indicating that 68% of MeOH generated was converted into DME. Then, the DME synthesis testing was conducted in the prototype-scale membrane reactor under the same conditions. As shown in Figure 7 (hollow column), DME

https://doi.org/10.1021/acs.iecr.2c02851
Ind. Eng. Chem. Res. 2022, 61, 14656−14663

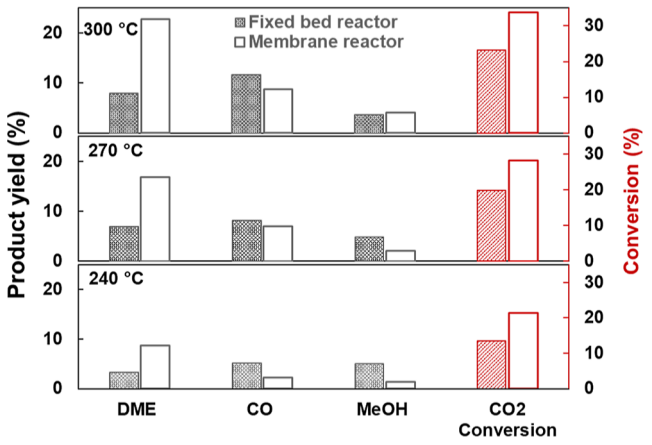

Figure 7. Comparison study between the traditional fixed bed reactor and membrane reactor.

yield increased from 8.71 to 22.8% when the operating temperature increased from 240 to 300 °C, while the CO_2 conversion increased from 21.4 to 33.7%, indicating that the conversion of MeOH (85 vs 68%) was increased significantly. Comparing with the fixed bed reactor, the CO_2 conversion increased by ∼45%, and the DME yield was around 2.9 times higher while employing the membrane reactor for DME synthesis, demonstrating the significant advantages of in situ water removal by membranes.

The influence of reaction conditions on the performance of the prototype membrane reactor for DME synthesis via CO_2 hydrogenation was investigated by carrying out the testing at different GHSVs [1400, 4200, and 8400 mL/(g·h)] and temperatures (240, 270, and 300 °C). The CO_2 conversion and DME yield increased with temperature under the same GHSV is shown in Table 1, which means that elevated temperature favored DME production. With GHSVs increased from 1400 to 4200 mL/(g·h) and further increased to 8400 mL/(g·h), the CO_2 conversion and DME yield were gradually decreased. This may result from the less resident time of feed gas in the catalyst bed.

Table 1. DME Synthesis Performance at GHSVs under Different Temperatures in the Fixed Bed Reactor and the Membrane Reactor

			yield (%)		
GHSVs [mL/(g·h)]	T (°C)	CO_2 conversion (%)	CO	DME	MeOH
1400 (fixed bed)	240	13.5	5.1	3.29	5.07
	270	19.9	8.12	6.94	4.86
	300	23.2	11.6	7.91	3.69
1400 (membrane reactor)	240	12.4	2.23	8.71	1.42
	270	26.0	7.04	16.9	2.04
	300	35.6	8.71	22.8	4.04
4200 (membrane reactor)	240	9.59	1.62	6.75	1.22
	270	19.7	5.37	12.5	1.83
	300	30.7	8.41	18.8	3.47
8400 (membrane reactor)	240	9.46	1.11	7.07	1.28
	270	16.1	3.65	10.5	1.96
	300	22.8	5.24	14.7	2.81

Figure 8 show the DME production rate as a function of GHSV at different temperatures. The DME production rate

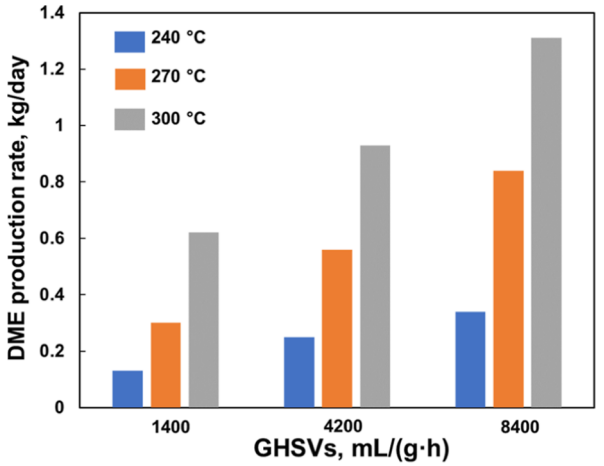

Figure 8. DME synthesis performance at different GHSVs under different temperatures.

increased with the increase of GHSVs at all the investigated temperatures. For example, the DME production rate increased from 0.34 to 0.84 and 1.31 kg/day when the GHSV increased from 1400 to 4200 and 8400 mL/(g·h) at the reaction temperate of 300 °C. Comparing with data in literature, this was the first time that DME was produced in scale of kilogram per day from one-step synthesis in a prototype membrane reactor.

4. CONCLUSIONS

In this work, a prototype-scale catalytic membrane reactor was first designed and constructed to investigate the DME production directly from CO_2 hydrogenation. A bifunctional CZZA/HZSM-5 bifunctional catalyst was employed for DME synthesis, and the water produced from the reaction was in situ removed by a highly efficient water selective NaA zeolite membrane. The DME yield and CO_2 conversion were increased from 8.71 and 21.4 to 22.8 and 33.7%, respectively. In the membrane reactor, the overall reaction performance was significantly improved, compared to the reaction with same operating conditions conducted in a conventional fixed bed reactor. Besides, DME production rate as high as 1.31 kg/day was achieved at 300 °C and 8400 mL/(g·h). Importantly, this approach of using a membrane reactor could also benefit the production of many other renewable chemicals and fuels.

AUTHOR INFORMATION

Corresponding Author

Shiguang Li − *Gas Technology Institute (GTI), Des Plaines, Illinois 60018, United States*; Email: SLi@gti.energy

Authors

Qiaobei Dong − *Gas Technology Institute (GTI), Des Plaines, Illinois 60018, United States*; orcid.org/0000-0001-9219-6319

Weiwei L. Xu − *Gas Technology Institute (GTI), Des Plaines, Illinois 60018, United States*

Xiao Fan − *Linda and Bipin Doshi Department of Chemical and Biochemical Engineering, Missouri University of Science and Technology, Rolla, Missouri 65409, United States*

https://doi.org/10.1021/acs.iecr.2c02851
Ind. Eng. Chem. Res. 2022, 61, 14656−14663

Huazheng Li − *Department of Chemical and Biological Engineering, University at Buffalo, Buffalo, New York 14260, United States*
Naomi Klinghoffer − *Gas Technology Institute (GTI), Des Plaines, Illinois 60018, United States*
Travis Pyrzynski − *Gas Technology Institute (GTI), Des Plaines, Illinois 60018, United States*
Howard S. Meyer − *Gas Technology Institute (GTI), Des Plaines, Illinois 60018, United States*
Xinhua Liang − *Linda and Bipin Doshi Department of Chemical and Biochemical Engineering, Missouri University of Science and Technology, Rolla, Missouri 65409, United States;* orcid.org/0000-0001-7979-0532
Miao Yu − *Department of Chemical and Biological Engineering, University at Buffalo, Buffalo, New York 14260, United States;* orcid.org/0000-0003-4730-7563

Complete contact information is available at: https://pubs.acs.org/10.1021/acs.iecr.2c02851

Author Contributions

Q.D. and W.L.X. contributed equally to this work. All authors have given approval to the final version of the manuscript.

Notes

The authors declare no competing financial interest.

■ ACKNOWLEDGMENTS

The authors gratefully acknowledge the support by the Department of Energy (DOE) Advanced Research Projects Agency-Energy (ARPA-E) under grant no. DE-AR0000806.

■ REFERENCES

(1) Datta, S. J.; Khumnoon, C.; Lee, Z. H.; Moon, W. K.; Docao, S.; Nguyen, T. H.; Hwang, I. C.; Moon, D.; Oleynikov, P.; Terasaki, O. CO_2 capture from humid flue gases and humid atmosphere using a microporous coppersilicate. *Science* **2015**, *350*, 302−306.
(2) Letcher, T. M. Global warming—a complex situation. In *Climate Change*; Elsevier, 2021; pp 3−17.
(3) Celik, S. The effects of climate change on human behaviors. In *Environment, Climate, Plant and Vegetation Growth*; Springer, 2020; pp 577−589.
(4) Davidson, D. J. Exnovating for a renewable energy transition. *Nat. Energy* **2019**, *4*, 254−256.
(5) Tian, Y.; Demirel, S. E.; Hasan, M. F.; Pistikopoulos, E. N. An overview of process systems engineering approaches for process intensification: State of the art. *Chem. Eng. Process.* **2018**, *133*, 160−210.
(6) Menghi, R.; Papetti, A.; Germani, M.; Marconi, M. Energy efficiency of manufacturing systems: A review of energy assessment methods and tools. *J. Cleaner Prod.* **2019**, *240*, 118276.
(7) Tapia, J. F. D.; Lee, J.-Y.; Ooi, R. E.; Foo, D. C.; Tan, R. R. A review of optimization and decision-making models for the planning of CO_2 capture, utilization and storage (CCUS) systems. *Sustain. Prod. Consum.* **2018**, *13*, 1−15.
(8) Sabri, M. A.; Al Jitan, S.; Bahamon, D.; Vega, L. F.; Palmisano, G. Current and future perspectives on catalytic-based integrated carbon capture and utilization. *Sci. Total Environ.* **2021**, *790*, 148081.
(9) Becattini, V.; Gabrielli, P.; Mazzotti, M. Role of carbon capture, storage, and utilization to enable a net-zero-CO_2-emissions aviation sector. *Ind. Eng. Chem. Res.* **2021**, *60*, 6848−6862.
(10) Catizzone, E.; Bonura, G.; Migliori, M.; Frusteri, F.; Giordano, G. CO_2 recycling to dimethyl ether: State-of-the-art and perspectives. *Molecules* **2017**, *23*, 31.
(11) Dieterich, V.; Buttler, A.; Hanel, A.; Spliethoff, H.; Fendt, S. Power-to-liquid via synthesis of methanol, DME or Fischer−Tropsch-fuels: a review. *Energy Environ. Sci.* **2020**, *13*, 3207−3252.
(12) Gulzar, A.; Gulzar, A.; Ansari, M. B.; He, F.; Gai, S.; Yang, P. Carbon dioxide utilization: A paradigm shift with CO_2 economy. *Chem. Eng. J. Adv.* **2020**, *3*, 100013.
(13) Makoś, P.; Słupek, E.; Sobczak, J.; Zabrocki, D.; Hupka, J.; Rogala, A. *Dimethyl Ether (DME) as Potential Environmental Friendly Fuel, E3S Web of Conferences*; EDP Sciences, 2019; p 00048.
(14) De Falco, M.; Capocelli, M.; Centi, G. Dimethyl ether production from CO_2 rich feedstocks in a one-step process: Thermodynamic evaluation and reactor simulation. *Chem. Eng. J.* **2016**, *294*, 400−409.
(15) Mondal, U.; Yadav, G. D. Perspective of dimethyl ether as fuel: Part I. Catalysis. *J. CO_2 Util.* **2019**, *32*, 299−320.
(16) Bonura, G.; Cordaro, M.; Cannilla, C.; Mezzapica, A.; Spadaro, L.; Arena, F.; Frusteri, F. Catalytic behaviour of a bifunctional system for the one step synthesis of DME by CO_2 hydrogenation. *Catal. Today* **2014**, *228*, 51−57.
(17) Akhoondi, A.; Osman, A. I.; Alizadeh Eslami, A. A. Direct catalytic production of dimethyl ether from CO and CO_2: A review. *Synth. Sintering* **2021**, *1*, 105−125.
(18) Ren, S.; Fan, X.; Shang, Z.; Shoemaker, W. R.; Ma, L.; Wu, T.; Li, S.; Klinghoffer, N. B.; Yu, M.; Liang, X. Enhanced catalytic performance of Zr modified CuO/ZnO/Al_2O_3 catalyst for methanol and DME synthesis via CO_2 hydrogenation. *J. CO_2 Util.* **2020**, *36*, 82−95.
(19) An, X.; Zuo, Y.-Z.; Zhang, Q.; Wang, D.-z.; Wang, J.-F. Dimethyl ether synthesis from CO2 hydrogenation on a CuO−ZnO−Al_2O_3−ZrO_2/HZSM-5 bifunctional catalyst. *Ind. Eng. Chem. Res.* **2008**, *47*, 6547−6554.
(20) Fan, X.; Jin, B.; Ren, S.; Li, S.; Yu, M.; Liang, X. Roles of interaction between components in CZZA/HZSM-5 catalyst for dimethyl ether synthesis via CO_2 hydrogenation. *AIChE J.* **2021**, *67*, No. e17353.
(21) Krim, K.; Sachse, A.; Le Valant, A.; Pouilloux, Y.; Hocine, S. One Step Dimethyl Ether (DME) Synthesis from CO2 Hydrogenation over Hybrid Catalysts Containing Cu/ZnO/Al_2O_3 and Nano-Sized Hollow ZSM-5 Zeolites. *Catal. Lett.* **2022**, 1−12.
(22) Fang, X.; Jia, H.; Zhang, B.; Li, Y.; Wang, Y.; Song, Y.; Du, T.; Liu, L. A novel in situ grown Cu-ZnO-ZrO_2/HZSM-5 hybrid catalyst for CO_2 hydrogenation to liquid fuels of methanol and DME. *J. Environ. Chem. Eng.* **2021**, *9*, 105299.
(23) Bonura, G.; Migliori, M.; Frusteri, L.; Cannilla, C.; Catizzone, E.; Giordano, G.; Frusteri, F. Acidity control of zeolite functionality on activity and stability of hybrid catalysts during DME production via CO_2 hydrogenation. *J. CO_2 Util.* **2018**, *24*, 398−406.
(24) Ortega, C.; Rezaei, M.; Hessel, V.; Kolb, G. Methanol to dimethyl ether conversion over a ZSM-5 catalyst: Intrinsic kinetic study on an external recycle reactor. *Chem. Eng. J.* **2018**, *347*, 741−753.
(25) Vu, T. T. N.; Desgagnés, A.; Iliuta, M. C. Efficient approaches to overcome challenges in material development for conventional and intensified CO_2 catalytic hydrogenation to CO, methanol, and DME. *Appl. Catal., A* **2021**, *617*, 118119.
(26) Ateka, A.; Ereña, J.; Bilbao, J.; Aguayo, A. s. T. Strategies for the intensification of CO_2 valorization in the one-step dimethyl ether synthesis process. *Ind. Eng. Chem. Res.* **2019**, *59*, 713−722.
(27) Diban, N.; Urtiaga, A. M.; Ortiz, I.; Ereña, J.; Bilbao, J.; Aguayo, A. T. Influence of the membrane properties on the catalytic production of dimethyl ether with in situ water removal for the successful capture of CO_2. *Chem. Eng. J.* **2013**, *234*, 140−148.
(28) Diban, N.; Urtiaga, A. M.; Ortiz, I.; Ereña, J.; Bilbao, J.; Aguayo, A. s. T. Improved performance of a PBM reactor for simultaneous CO_2 capture and DME synthesis. *Ind. Eng. Chem. Res.* **2014**, *53*, 19479−19487.
(29) Iliuta, I.; Larachi, F.; Fongarland, P. Dimethyl ether synthesis with in situ H_2O removal in fixed-bed membrane reactor: model and simulations. *Ind. Eng. Chem. Res.* **2010**, *49*, 6870−6877.
(30) Rieck genannt Best, F.; Mundstock, A.; Kißling, P. A.; Richter, H.; Hindricks, K. D.; Huang, A.; Behrens, P.; Caro, J. r. Boosting

Dimethylamine Formation Selectivity in a Membrane Reactor by In Situ Water Removal. *Ind. Eng. Chem. Res.* **2021**, *61*, 307−316.
(31) Raso, R.; Tovar, M.; Lasobras, J.; Herguido, J.; Kumakiri, I.; Araki, S.; Menéndez, M. Zeolite membranes: Comparison in the separation of $H_2O/H_2/CO_2$ mixtures and test of a reactor for CO_2 hydrogenation to methanol. *Catal. Today* **2021**, *364*, 270−275.
(32) Li, Z.; Deng, Y.; Dewangan, N.; Hu, J.; Wang, Z.; Tan, X.; Liu, S.; Kawi, S. High temperature water permeable membrane reactors for CO_2 utilization. *Chem. Eng. J.* **2021**, *420*, 129834.
(33) Brunetti, A.; Migliori, M.; Cozza, D.; Catizzone, E.; Giordano, G.; Barbieri, G. Methanol conversion to dimethyl ether in catalytic zeolite membrane reactors. *ACS Sustainable Chem. Eng.* **2020**, *8*, 10471−10479.
(34) Poto, S.; Gallucci, F.; d'Angelo, M. F. N. Direct conversion of CO_2 to dimethyl ether in a fixed bed membrane reactor: Influence of membrane properties and process conditions. *Fuel* **2021**, *302*, 121080.
(35) Rohde, M.; Schaub, G.; Khajavi, S.; Jansen, J.; Kapteijn, F. Fischer−Tropsch synthesis with in situ H_2O removal−Directions of membrane development. *Microporous Mesoporous Mater.* **2008**, *115*, 123−136.
(36) Ateka, A.; Rodriguez-Vega, P.; Cordero-Lanzac, T.; Bilbao, J.; Aguayo, A. T. Model validation of a packed bed LTA membrane reactor for the direct synthesis of DME from CO/CO_2. *Chem. Eng. J.* **2021**, *408*, 127356.
(37) Koybasi, H. H.; Avci, A. K. Modeling of a membrane integrated catalytic microreactor for efficient DME production from syngas with CO_2. *Catal. Today* **2022**, *383*, 133−145.
(38) Rodriguez-Vega, P.; Ateka, A.; Kumakiri, I.; Vicente, H.; Ereña, J.; Aguayo, A. T.; Bilbao, J. Experimental implementation of a catalytic membrane reactor for the direct synthesis of DME from H_2+ CO/CO_2. *Chem. Eng. Sci.* **2021**, *234*, 116396.
(39) Dong, Q.; Jiang, J.; Li, S.; Yu, M. Molecular layer deposition (MLD) modified SSZ-13 membrane for greatly enhanced H_2 separation. *J. Membr. Sci.* **2021**, *622*, 119040.
(40) Choi, J.; Jeong, H.-K.; Snyder, M. A.; Stoeger, J. A.; Masel, R. I.; Tsapatsis, M. Grain boundary defect elimination in a zeolite membrane by rapid thermal processing. *Science* **2009**, *325*, 590−593.
(41) Li, H.; Qiu, C.; Ren, S.; Dong, Q.; Zhang, S.; Zhou, F.; Liang, X.; Wang, J.; Li, S.; Yu, M. Na^+-gated water-conducting nanochannels for boosting CO_2 conversion to liquid fuels. *Science* **2020**, *367*, 667−671.
(42) Li, H.; Ren, S.; Zhang, S.; Padinjarekutt, S.; Sengupta, B.; Liang, X.; Li, S.; Yu, M. The high-yield direct synthesis of dimethyl ether from CO_2 and H_2 in a dry reaction environment. *J. Mater. Chem. A* **2021**, *9*, 2678−2682.

https://doi.org/10.1021/acs.iecr.2c02851
Ind. Eng. Chem. Res. 2022, 61, 14656−14663